IJREAT International Journal of Research in Engineering & Advanced Technology, Volume 5, Issue 3, June - July, 2017
ISSN: 2320 – 8791 (Impact Factor: 2.317)
www.ijreat.org

A Novel Image Enhancement Technique Using Interpolation-Based Method

Santhosh Gupta Dogiparthi[1], JagadeeshThati[2], V. Anil Kumar[3]

[1,3] *Assistant Professor, Department of ECE ,Tirumala Engineering College, Jonnalagadda, Narasaraopet.*
[2] *Associate Professor, Department of ECE, Tirumala Engineering College, Jonnalagadda, Narasaraopet.*

***Abstract*—The digital image processing has been applied in several areas, especially where it is necessary to use tools for feature extraction.In this paper, we propose a new interpolation-based method of image super-resolution reconstruction. A coarse version of the input image is first in painted by a non- parametric patch sampling. From the low-resolution in painted image, a single-image super-resolution is applied to recover the details of missing areas. The idea is using multi-surface fitting to take full advantage of spatial structure information. Each site of low-resolution pixels is fitted with one surface, and the final estimation is made by fusing the multisampling values on these surfaces in the maximum *a posteriori* fashion. With this method, the reconstructed high-resolution images preserve image details effectively without any hypothesis on image prior. Furthermore, we extend our method to a more general noise model.**

Index Terms—Data fusion, multi-surface fitting, non-uniform interpolation, super-resolution (SR).

I. INTRODUCTION

Image super-resolution (SR) has been extensively studied to solve the problem of limited resolution in imaging devices for decades [1], [2]. It has wide applications in video surveillance, remote imaging, medical imaging, etc. The idea of SR is to reconstruct a high-resolution (HR) image from aliased low-resolution (LR) images. There are four main classes of methods to estimate the pixel values in HR grids, i.e., frequency-domain approaches, learning-based approaches [3], iterative HR image reconstruction techniques [5], [6], and interpolation-based approaches [6]–[9], [10]. Some literature works [2] consider the filtering approaches as a separate class, but in this paper, they are included in interpolation-based approaches since both interpolation and filtering can be expressed in the form of a weighted sum. Frequency-domain approaches make explicit use of the aliasing relation between continuous Fourier transform and discrete Fourier transform [4]. However, this kind of SR approaches is only restricted to global translational motion and linear space-invariant blur. Learning-based approaches embed more information into LR images from learning examples. The embedded information can be utilized to relate LR and HR image patches [7], choose the reconstruction parameters [8], etc. However, neither of the approaches in [7] and [8] represents the image co-occurrence knowledge in an effective way. Thus, their performances largely depend on the learning examples. To cope with this problem, Yang *et al.* present a method based on the sparse association between input and example patches [3]. Nevertheless, it does not take into account geometric image structures that play an important role in the choice of example patches. Moreover, the increase in resolution in the learning-based approaches is limitedby the resolution of learning examples. Among iterative HR image reconstruction techniques, the most popular ones are the projection on convex sets algorithm [6], the maximum *a posteriori* (MAP) estimation [5], and their variations. The main advantage of them is that it is convenient to add image priors. To regularize the ill-posed inverse problem, [7] utilizes the total variation function as the image prior. This prior is conducive to preserve the edge, i.e., image structures of one order. However, the choice of model parameters remains unsolved. A variational approach is proposed in [10] to address this problem by using a two-level Bayesian inference.

A further work based on this idea suggests incorporating registration information as another prior [10]. With the help of constraints or regularization, most iterative methods perform well. However, they are, in general, computationally expensive and high-order image structures are not considered. Interpolation-based approaches generally treat SR as a non-uniform interpolation problem. They are usually intuitive and computationally efficient. In [10], interpolation is implemented as a pixel wise average algorithm of the LR measurements. Meanwhile, regularization of a bilateral filter is introducedfor edge

preservation. Consequently, the local spatialstructure information is severely lost. The interpolation-based approachusing Delaunay triangulation is first addressed in [3], whose idea is tomodel each triangle patch as a bivariate polynomial. The method in [9]suggests a sampling theory framework with an anti-aliasing pre-filter, where the sampled coefficients are calculated by integrating B-splinepolynomials and Delaunay triangles. Although Delaunay triangulation expresses spatial structures implicitly and partially, it does not utilizethe structure information effectively [9]. Furthermore, it is expensiveto structure the tessellation with respect to both the memory spaceand computationaltime.

II. SUPER-RESOLUTION ALGORITHM

Once the in painting of the low-resolution picture is completed, a single-image super-resolution approach is used to reconstruct the high resolution of the image. The idea is to use the low-resolution in painted areas in order to guide the texture synthesis at the higher resolution. The problem is to find a patch of higher-resolution from a database of examples.

1. Dictionary building: it consists of the correspondences between low and high resolution image patches. The unique constraint is that the high-resolution patches have to be valid, i.e. entirely composed of known pixels. In the proposed approach, high-resolution and valid patches are evenly extracted from the known part of the image. The size of the dictionary is a user-parameter which might influence the overall speed/quality trade-off. An array is used to store the spatial coordinates of HR patches (DHR). Those of LR patches are simply deduced by using the decimation factor.
2. Filling order of the HR picture: It is computed on the HR picture with the sparsity-based method. This improves the quality of the in painted picture compared to a raster-scan filling order.
3. For the LR patch corresponding to the HR patch having the highest priority, its K-NN in the in painted images of lower resolution are sought. The number of neighbors is computed as described in the previous section. The similarity metric is also the same as previous one.
4. Weights wp, pj are calculated by using a non-local means method as if we would like to perform a linear combination of these neighbors. However, the similarity distance used to compute the weights is composed of two terms: the first one is classical since this is the distance between the current LR patch and its LR neighbors, noted d (LRp, LRp, pj). The second term is the distance between the known parts of the HR patch HRp and the HR patches corresponding to the LR neighbors of LRp. Say differently, the similarity distance is the distance between two vectors composed of both pixels of LR and HR patches. The use of pixel values of HR patches allows to constraint the nearest neighbor search of LR patches.
5. A HR candidate is finally deduced by using a linear combination of HRpatches with the weights previously computed:

HRp =Xpj2DHRwp, pj× p, pj (4)

With the usual conditions $0 \leq$ wp, pj ≤ 1, and

wp,pk = 1.

6. Stitching: The HR patch is then pasted into the missing areas. However, as an overlap with the already synthesized areas is possible, a seam cuttingthe overlapped regions is determined to further enhance the patch blending. The minimum error boundary cut is used to find a seam for which the two patches match best. The similarity measure is the Euclidean distance between all pixel values in the overlapping region.

III. PROPOSED METHOD

In this section, we first introduce the overall framework and the mathematical notations therein, and then present the specific implementation of our algorithm for SR. At the end of this section, the proposed method is extended to a more general noise model.

A. System Overview

Essentially, the problem of interpolation-based SR is how to convert arbitrarily sampled data to evenly spaced data [1]. After sub pixel registration, pixels from different observed LR images are positioned in an HR grid, as shown in Fig. 1.

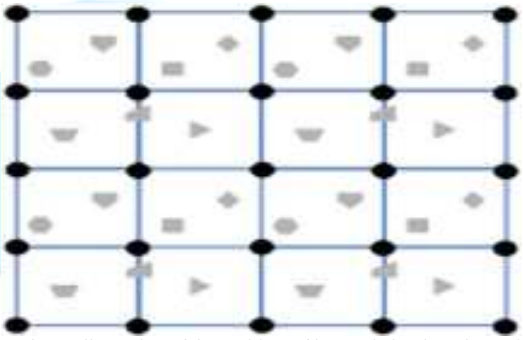

Fig. 1. Illustration of the problem of interpolation-based SR.The "circles" grid nodes represent the HR pixels to be estimated. The LR pixels are represented by other shapes. Different shapes represent pixels from different LR images.

Suppose that the intensity of the HR pixel $p_H$is the value to be estimated. In the neighborhood of HR pixels, we have different LR pixels denoted by $p_{L1} \ldots\ldots p_{Li} \ldots. p_{LK}$ where K is the number of LR pixels in the neighborhood of p_H.

A conventional idea is to fit a surface with local smoothness from a group of LR pixels

$(p_{L1} \ldots . p_{Li} \ldots . p_{LK})$. The fitted surface can be regarded as the continuous image. Subsequently, the HR pixel p_H is obtained by resampling the surface. This process can be formulated as$\Gamma = \Gamma(f(p_{L1}) \ldots . f(p_{Li}) \ldots . f(p_{LK}),$

$x_{L1} \ldots . x_{Li} \ldots . x_{Lk}, y_{L1} \ldots . y_{Li} \ldots . y_{Lk})$ (1)$f(p_H) = S(x_H . y_H . \Gamma)$ (2)

where Γ represents the fitted surface for multipixels, $f(p_\phi)$is theintensity of pixel p_ϕ, x_ϕ and $y_\phi$indicate the location of pixel $p_\phi$inabscissa and ordinates of the HR grid, respectively; $S(x_\phi, y_\phi, \Gamma)$is an operation of sampling the surface Γ at location(x_ϕ, y_ϕ); and$\phi \epsilon \{H, L1, Li, Lk\}$. In (1), all the LR pixels are regardedas equivalent ones with the same noise and error. Moreover, spatialstructure information is not sufficiently considered. In our view, thespatial structures in the HR grid should comprise two aspects. Oneis the spatial distributions of LR pixels in the HR grid. The other isthe local structures of intensity, i.e., edge orientations, curvatures, etc.The former can be represented by the positions of LR pixels in thecoordinate system of the HR grid, and the later can be denoted byintensity derivatives of different orders.Considering the difference of LR pixels, we first fit one surface ateach site of LR pixels. Hence, there is a one-to-one correspondence between fitted surfaces and LR pixels.

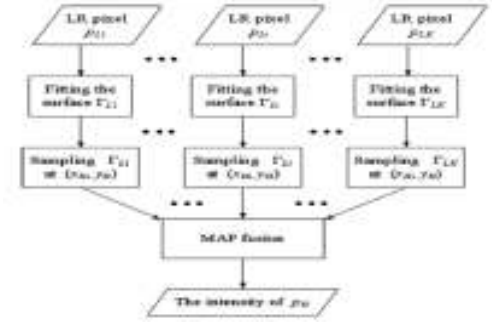

Fig. 2.Flowchart for estimating the intensity of HR pixel p_H in our method. The inputs are LR pixels, including their positions and intensities. The output is the intensity of p_H .

Then, we can obtain a series of intensity values at the location of pixel p_ϕ by sampling all K surfaces, i.e.,

$$f_{Li}(p_\phi) \triangleq S(x_\emptyset . y_\emptyset . \Gamma_{Li}), 1 \le i \le K \quad (3)$$

WhereΓ_{Li} is the fitted surface for pixel p_{Li}. It should be noticed that Γ_{Li} and Γ have different meanings. The final intensity of p_H can be calculated by MAP estimation, i.e.,

$$\hat{f}(p_H) = \arg\max q(f(p_H)|f_{L1}(p_H), \ldots, f_{Lk}(p_H)) = \arg\max q\left(f_{L1}(p_H), \ldots, (f_{Lk}(p_H)|f(p_H))\right) q(f(p_H)) \quad (4)$$

Where $q(\cdot)$denotes the probability density function. The above idea is illustrated in Fig. 2.

B. Implementation for SR

In this section, we will describe how to embody the formulas ofΓ_{Li} and (4), respectively. To take advantage of spatial structure information sufficiently, we prefer to construct surfaces using 2-D Taylor series, e.g., surfaceΓ_{Li} is given by

$$\begin{aligned}\Gamma_{Li} = \Gamma_{Li}(x, y) \quad &= f(p_{Li}) + \frac{\partial f(p_{Li})}{\partial x}(x - x_{Li}) \\ &+ \frac{\partial f(p_{Li})}{\partial y}(y - y_{Li}) \\ &+ \frac{\partial^2 f(p_{Li})}{2 \cdot \partial x^2}(x - x_{Li})^2 \\ &+ \frac{\partial^2 f(p_{Li})}{2 \cdot \partial y^2}(y - y_{Li})^2 \\ &+ \frac{\partial^2 f(p_{Li})}{\partial x \partial y}(x - x_{Li})(y - y_{Li}) + \cdots \quad (5)\end{aligned}$$

Where$x$ and y are the arguments of functionΓ_{Li}, denoting the locations in the HR grid. In (5), intensity derivatives of LR pixel p_{Li}can beconsidered as the parameters of surface Γ_{Li}.A naive method is to estimate these derivatives in LR images, but it is coarse in the context of SR. In this paper, we utilize the following equations to estimate them:

$$f(p_{Lj}) = f_{Li}(p_{Lj}) + \xi_{ij}, \quad 1 \le i \le K, 1 \le j \le M_i \quad (6)$$

Wherep_{Lj} an LR pixel in the neighborhood of isp_{Li}, $M_i$is the number of LR pixels in the neighborhood of $p_{Li}$and$\xi_{i\,j}$is the error of the surface Γ_{Li}at the location of pixelp_{Lj}. Under the smoothness assumptionof estimated HR image, $\xi_{i\,j}$is 0 ideally. Thus, according to (3), (5), and (6), we have $1 < j < M_i, \Delta x_{j,i} = x_{L\,j} - x_{L\,i}, \Delta y_{j,i} = x_{L\,j} - x_{L\,i}$and $\Delta f_{j,i} = f(p_{L\,j}) - f(p_{L\,i})$. In order to obtain reliable and valid solutions, (7) should be over determined. After plugging the least square solutions of (7) back into (5) to obtain the explicit surface, we have two important findings.

$$\begin{bmatrix} \Delta x_{1,i} & \Delta y_{1,i} & \frac{\Delta x_{1,i}^2}{2} & \frac{\Delta y_{1,i}^2}{2} & \Delta x_{1,i} \cdot \Delta y_{1,i} \\ \vdots & \vdots & \vdots & \vdots & \vdots \\ \Delta x_{j,i} & \Delta y_{j,i} & \frac{\Delta x_{j,i}^2}{2} & \frac{\Delta y_{j,i}^2}{2} & \Delta x_{j,i} \cdot \Delta y_{j,i} \\ \vdots & \vdots & \vdots & \vdots & \vdots \\ \Delta x_{k,i} & \Delta y_{k,i} & \frac{\Delta x_{K,i}^2}{2} & \frac{\Delta y_{K,i}^2}{2} & \Delta x_{K,i} \cdot \Delta y_{K,i} \end{bmatrix} \times \begin{bmatrix} \frac{\partial f(p_{Li})}{\partial x} \\ \frac{\partial f(p_{Li})}{\partial y} \\ \frac{\partial^2 f(p_{Li})}{\partial x^2} \\ \frac{\partial^2 f(p_{Li})}{\partial y^2} \\ \frac{\partial^2 f(p_{Li})}{\partial x \partial y} \end{bmatrix} = \begin{bmatrix} \Delta f_{1,i} \\ \vdots \\ \Delta f_{j,i} \\ \vdots \\ \Delta f_{K,i} \end{bmatrix} \quad (7)$$

First, spatial structures are retained, includingedge orientations (first-order derivatives) and curvatures (second-orderderivatives), etc. Second, the levels of retained details depend on thenumber of LR pixels in the neighborhood. More LR pixels tend to producemore details, which are highly consistent with

intuitions. Specifically, first-order derivatives can be retrieved if $M_i > 3$, second-orderderivatives can be retrieved if $M_i > 6$, etc. An associated problem isthe choice of neighborhood of $p_{L\,i}$, which determines the value of M_i.On one hand, from (7), we wish to have as many LR pixels as possible.On the other hand, from (5), it is obvious that $\Delta x_{j,i}$and$\Delta y_{j,i}$ shouldbe less than 1.Hence, the size of neighborhood is chosen as 1 X 1 HRpixel. Once surfaceΓ_{Li} is obtained, $\xi_{i\,j}$can be calculated from (6). Whensurface $\Gamma_{Li}$is utilized to estimate$f(p_H)$, the variance σ_i^2 of fittingerrors can be calculated as

$$\sigma_i^2 = \frac{1}{M_i}\sum_{j\neq i}(\xi_{ij})^2 \cdot \qquad (8)$$

Under Gaussian assumption, (4) becomes

$$\hat{f}(p_H) = \arg\min f(p_H)\left[\sum_{i=1}^{K}\frac{\left|(f_{Li}(p_H) - f(p_H))^2\right|}{\sigma_i} + \lambda(f_0(p_H) - f(p_H))^2\right] \qquad (9)$$

where$f_0(p_H)$is the prior estimation of $f(p_H)$ and is an empirical parameter.

The prior estimation can be obtained using either a B-spline interpolation or a simple SR reconstruction. Let the gradient of the cost in (9) be equal to zero, we get the MAP estimation for the intensity of the HR pixel p_H

$$\hat{f}(p_H) = \frac{1}{\lambda + \sum_{i=1}^{K}\lambda_i}\left(\lambda f_0(p_H) + \sum_{i=1}^{K}\lambda_i f_{Li}(p_H)\right) \qquad (10)$$

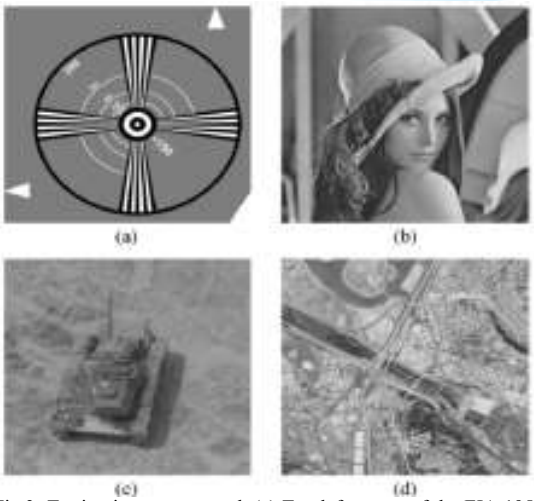

Fig.3. Testing images we used. (a) Top left corner of the EIA 1956 video resolution target or "part of EIA" for short. (b) Lena. (c) Tank. (d) Aerial image of San Diego.

Where $\lambda_i = \frac{1}{\sigma_i^2}$. Since the expression in (10) has the form of a weighted sum, the proposed method is an interpolation-based approach. Essentially, the weights for the surfaces depend on the agreement of other LR pixels.

C. Algorithm to estimate the intensity of HR pixels

Given registered LR images set the size of neighborhood to 1. Forevery HR pixel to be estimated

1) Search the LR pixels that are located in the neighborhood of the HR pixel. Count the number of LR pixels, denoted as K. If K is equal to zero, increase the size of neighborhood and repeat step 1.
2) According to the value of K, estimate parameters (derivatives of different orders) for every surface (LR pixel) using (7).
3) Estimate $\xi_{i\,j}$ using (5), (6), and the derivatives calculated in the previous step.
4) Estimate $\lambda_i = \frac{1}{\sigma_i^2}$. Using (8).
5) Estimate the HR pixel value using (3) and (10).

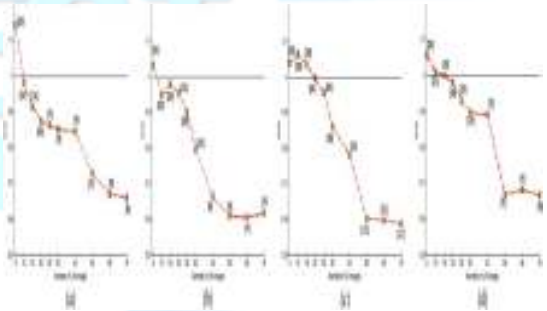

Fig. 4. Quantitative comparisons based on MSE. (a) Part of EIA. (b) Lena. (c) Tank. (d) Aerial image of San Diego. The words near the square markers indicate the method with the lowest MSE.

D. Extension

The above analysis is based on the conventional assumption of Gaussian noise. However, the Laplacian distribution is more appropriate to describe the noise for real word sequences in the context of SR. In this case, (8) and (9), respectively, become

$$\sigma_i = \frac{1}{M_i}\sum_{j\neq i}|\xi_{ij}| \qquad (11)$$

$$\hat{f}(p_H) = \arg\min f(p_H)\left[\sum_{i=1}^{K}\frac{\left|(f_{Li}(p_H) - f(p_H))\right|}{\sigma_i} + \beta|f_0(p_H) - f(p_H)|\right] \qquad (12)$$

Whereβ has the same meaning as λ in (9). In our experiments, we have obtained satisfying results by simply setting both λ and β to zero. The gradient term of the cost in (12) is

$$\sum_{i=1}^{K} sign\left(\beta_i\left(f_{Li}(p_H) - f(p_H)\right) + \beta \cdot \left(f_0(p_H) - f(p_H)\right)\right) \quad (13)$$

Where $\beta_i = \frac{1}{\sigma_i}$.

The effect of the sampling values has one of the following three forms.

- Addition of zero, which results from indiscrimination.
- Addition of $+\beta_i$, which means that f(p_H) was smaller than sampling value$f_{Li}(pH)$.
- Addition of$-\beta_i$, which means that f (p_H) was larger than sampling value$f_{Li}(pH)$.

Obviously, a zero state of gradient term can be obtained by adding or subtracting different weights. Consequently, (13) essentially is the weighted median filter. Since the framework remains unchanged, the algorithm for Laplacian noise has the similar steps as the one in the previous section except steps 4 and 5. In step 4, we should replace (8) by (11). Likewise, in step 5, we adopt the weighted median filter instead of (10).

IV. RESULTS AND DISCUSSION

In this section, extensive simulations were carried out on four well-known images, which are shown in Fig. 3. Fig. 3(a) is the top left corner of the EIA 1956 video resolution target, and Fig. 3(b)–(d) are from the USC-SIPI image database [1]. The resolution of all these images is 512 X 512. In our simulations, the images were corrupted by Gaussian noise with signal-to-noise ratio (SNR) of 15 dB. Accordingly, we adopt the proposed algorithm, which is derived from Gaussian assumption. Different LR images were generated through fourfold down sampling. The positions of sampling are random, following a uniform distribution between zero and one LR pixels. The number of LR images, which are used in reconstruction, is varied. We have utilized 5, 15, 20, 25, 30, 40, 50, 60, and 70 LR images, respectively. In all the implementations, only sensor blur is taken into consideration. In order to quantify the reconstruction results, we use mean square error (MSE).

The SR reconstruction is believed to be more accurate if lower MSE is obtained. We have summarized the results in Fig. 4, where the abscissa is the number of LR images used in SR reconstructions and the ordinate is the ratio of the MSE of our method over the lowest MSE of the methods in [9]–[10], and . In Fig. 4, we can see that our proposed SR reconstruction method achieves lower MSE in most cases.

Although our method may be inferior when the number of LR images is small, it performs superior as the number of LR images increases. Specifically, our method performs best when the number of LR images is more than 15 and the superiority of our method becomes more obvious as the number of LR images increases from 15 to 50. These experimental results can be interpreted as follows. On one hand, when the number of LR images is small, only zero-order derivatives can be retrieved, and (5) and (8) become inaccurate. To cope with this problem, one can incorporate some additional information such as noise level and registration error (not included in this paper).

On the other hand, for simplicity, we only consider second-order derivatives in the implementation of our method. About 50 LR images are sufficient to retrieve second-order derivatives precisely in our experiments. More LR images are necessary for high-order derivatives but may be redundant for the second-order. In addition to MSE, another metric, known as visual information fidelity (VIF) is attractive for image quality assessments. In this metric is reported to be consistent with subjective human evaluation. A larger VIF means a better result of reconstruction. If VIF reaches 1, the "perfect" reconstruction is achieved. We further utilize it to demonstrate the superiority of our method in the case of sufficient LR images. To calculate the VIF of a testing image, a reference image is necessary.

In this paper, the original HR images serve as the reference images. However, as the number of LR images increases regularization becomes trivial and ignores the underlying information of the spatial structures in the HR grid.

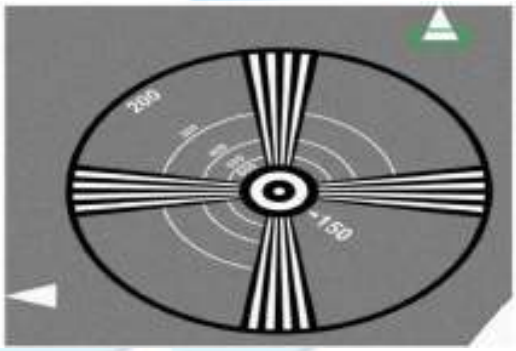

(a)

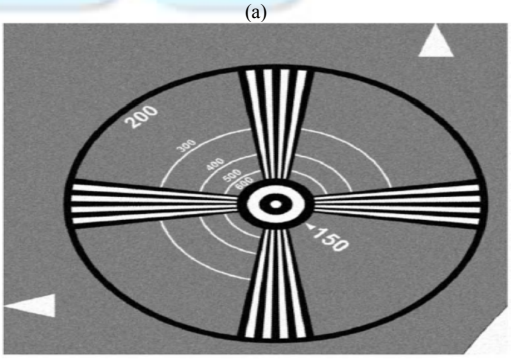

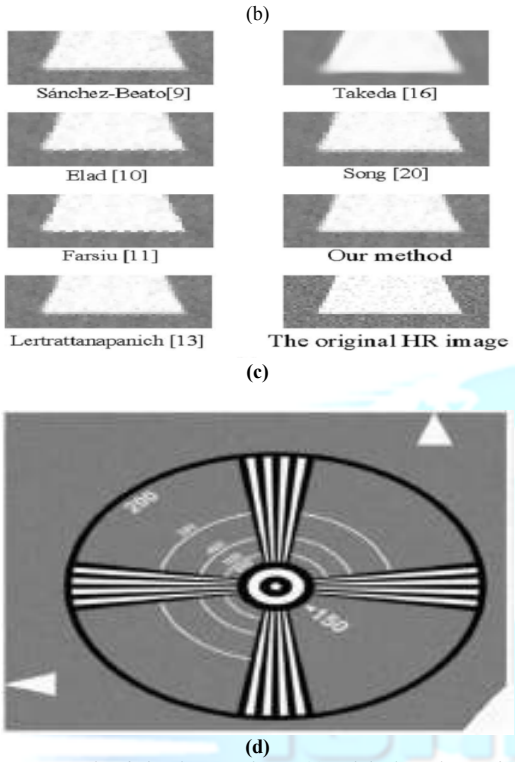

Fig. 5.Example of visual comparisons. (a) Original HR image from Fig. 3(a) with Gaussian noise of 15-dB SNR. (b) Result of our method using 25 LR images.(c) Details comparison for the highlighted patch in Fig. 5(a). (d) Result using 25 LR images.

According to the above analysis, we get the conclusion that our method is particularly efficient for the applications with large amounts of observed images, e.g., traffic surveillance and remote sensing. We also give a visual example in Fig. 5 to illustrate the superiority of our method. The SR result of our method is shown in Fig. 5(b).

In order to compare our method with other SR methods intuitively, we illustrate a comparison of details in Fig. 5(c), where all the SR methods using the same 25 LR images reconstruct an HR image. In Fig. 5(c), we can observe that our method generates fewer artifacts than the compared methods in [9]–[10] and [2]. Although the method in [1] can produce smooth edges, it leads to the results of more blurring. This may be obvious in some fine-grained regions. For example, we can recognize all the numeric characters in Fig. 5(b) whereas some small ones cannot be distinguished in Fig. 5(d). In addition to image quality, the elapsed time is also an important evaluation indicator for image SR. We have enumerated the average run time.

Our method is computationally efficient compared with some counterparts, although its run time is not the lowest. Since our method is performed in the pixel wise style, it is worthwhile to note that it can be accelerated if parallel implementations are adopted.

V. Conclusion

In this paper, we have presented an image SR reconstruction framework using multisurface fitting. It creates one surface for every LR pixel. These surfaces can effectively retain the image details such as image gradients, curvatures, or even higher order information. Each surface has different weights in estimation of the HR intensity values. In the MAP frame, the surfaces with smaller noise and errors tend to have greater contributions. We also extend our method to the more general laplacian model by introducing the weighted median filter. Moreover, our method is pixel wise and non-iterative. Hence, it does not suffer from convergence problems and can be accelerated through parallel implementations. Experimental results demonstrate the superiority and potential applications of our method.

REFERENCES

[1] A. K. Katsaggelos, R. Molina, and J. Mateos, *Super Resolution of Images and Video*. San Rafael, CA: Morgan & Claypool, 2007.

[2] S. C. Park, M. K. Park, and M. G. Kang, "Super-resolution image reconstruction: A technique overview," *IEEE Signal Process. Mag.*, vol. 20, no. 3, pp. 21–36, May 2003.

[3] J. Yang, J. Wright, Y. Ma, and T. S. Huang, "Image super-resolutionvia sparse representation," *IEEE Trans. Image Process.*, vol. 19, no. 11,pp. 2861–2873, Nov. 2010.

[4] T. S. Huang and R. Y. Tsai, "Multi-frame image restoration and registration, *"Adv. Compute. Vis. Image Process.*, vol. 1, pp. 317–339, 1984.

[5] R. R. Schulz and R. L. Stevenson, "Extraction of high-resolutionframes from video sequences," *IEEE Trans. Image Process.*, vol. 5, no. 6, pp. 996–1011, Jun. 1996.

[6] A. J. Patti, M. I. Sezan, and A. M. Tekalp, "Super resolutionvideo reconstruction with arbitrary sampling lattices and nonzero aperture time," *IEEE Trans. Image Process.*, vol. 6, no. 8, pp. 1064–1076, Aug.1997.

[7] W. T. Freeman, T. R. Jones, and E. Z. Pasztor, "Example-based superresolution,"*IEEE Comput. Graph. Appl.*, vol. 22, no. 2, pp. 56–65, Mar. 2002.

[8] B. Narayanan, R. C. Hardie, K. E. Barner, and M. Shao, "A computationally efficient super-resolution algorithm for video processing using partition filters," *IEEE Trans. Circuits Syst. Video Technol.*, vol. 17, no.5, pp. 621–634, May 2007.

[9] A. Sánchez-Beato and G. Pajares, "Noniterative interpolation-basedsuper-resolution minimizing aliasing in the reconstructed image,"*IEEE Trans. Image Process.*, vol. 17, no. 10, pp. 1817–1826, Oct.2008.

[10] M. Elad and Y. Hel-Or, "A fast super-resolution reconstruction algorithm for pure translational motion and common space invariant blur,"*IEEE Trans. Image Process.*, vol. 10, no. 8, pp. 1187–1193, Aug. 2001.

Mr. Santhosh Gupta Dogiparthi received his B.Tech (ECE) degree from Amara Institute of Engineering and technology affiliated to JNTU, Kakinada and M.Tech (DSCE) degree fromNarasaraopeta Engineering College, Narasaraopet, Guntur District, Andhra Pradesh, India.Presently , Working as an Assistant Professor since December 2014 in Tirumala Engineering College, Jonnalagadda. His area of interests include Image Processing, Embedded Systems and Communications.

Mr. JagadeeshThati is currently working as Associate Professor in Department of ECE at Tirumala Engineering College, Jonnalagadda, Narasaraopet, Guntur (dt). He has worked as dasa5 developer in Dasa Control systems AB Hammerdalsvgen 3, SE-352 46 Vxjo, Sweden. He did his MS from BTH, Sweden. He has published 23 international journals, 8 international conferences and two Books. He has appointed as reviewer for various journals. He has professional memberships in IETE and ISTE.He received best Teacher award from Tirumala Engineering College in 2012. His areas of Interests are Signal Processing, Digital Image Processing, Computer Vision, Neural Networks and Nano Technology.

Mr. V. Anil Kumar received his B.Tech (ECE) degree from Nalanda Institute of Engineering and technology affiliated to JNTU, Kakinada and M.Tech (CSP) degree fromBapatla Engineering College, Bapatla, Guntur District, Andhra Pradesh, India.Presently, Working as an Assistant Professor since June 2015 in Tirumala Engineering College, Jonnalagadda. His area of interests include Signal and Image Processing.